

---

# Estimation of Dopamine D2 Receptor Binding Potential in the Striatum with Iodine-123-IBZM SPECT: Technical and Interobserver Variability

Nicolaas P.L.G. Verhoeff, Ozlem Kapucu, Ellinor Sokole-Busemann, Eric A. van Royen and Antonius G.M. Janssen

*Department of Nuclear Medicine, Academic Medical Centre, Amsterdam and Cygne B.V., Technical University, Eindhoven, The Netherlands*

---

Factors contributing to the quantification of the striatal dopamine D2 receptor binding potential in vivo using  $^{123}\text{I}$ -iodobenzamide ( $^{123}\text{I}$ -IBZM) and SPECT were analyzed in phantom studies, healthy volunteers and in patients with the parkinsonian syndrome. A cylindrical brain phantom based on a stereotactic brain atlas was constructed with independently fillable compartments representing two striata (ST), cerebellum (CB) and background. Clinical  $^{123}\text{I}$ -IBZM SPECT studies were performed on 15 healthy volunteers and on 28 patients with parkinsonian syndrome. Interobserver variability of region of interest (ROI) selection and count ratios were estimated by two independent observers. ROIs for the striatum were either fixed, based on a stereotactic brain atlas, or drawn manually, based on 70% isocontour lines. Reference regions were either the cerebellum (isocontour ROIs) or the occipital cortex (occipital cortex; fixed ROIs). The brain phantom measurements showed linearity with respect to radioactivity concentration, good reproducibility and good contrast recovery. The interobserver study showed that the striatum-to-occipital cortex ratio with fixed ROIs for the striatum, as an estimate for striatal D2 receptor binding potential, resulted in a means of separating patients with normal receptor activity from those with decreased striatal dopamine D2 receptor activity.

**J Nucl Med 1993; 34:2076–2084**

---

**I**odine-123-labeled (S)-2-hydroxy-6-methoxy-N-((1-ethyl-2-pyrrolidinyl)methyl) benzamide ( $^{123}\text{I}$ -IBZM) is a recently developed, highly specific dopamine D2 receptor ligand suitable for measuring striatal receptor activity by SPECT. This agent demonstrates specific binding to dopamine D2 receptors in vitro and in vivo (1–5).

Differential diagnosis of parkinsonian symptoms is important in view of differences in prognosis and therapy between idiopathic Parkinson's disease (IPD) and diseases such as multiple system atrophy (MSA) and progressive supranuclear palsy (PSP) (6). The study of postsynaptic dopamine D2 receptors in vivo appears to be helpful in this

respect. The dopamine D2 receptor binding potential in the striatum is presumed to be normal or slightly elevated in IPD and to be decreased in both MSA and PSP (6–9). Therefore, SPECT with  $^{123}\text{I}$ -IBZM may be a useful alternative to PET for discrimination of diseased versus healthy individuals (10).

Interobserver reliability studies of the measurement of the striatal dopamine D2 receptor binding potential with SPECT have not been reported. Count ratios based on different reference regions within brain SPECT images have been used to estimate dopamine D2 receptor binding potential in the striatum. Both the cerebellum (2, 7) and the frontal cortex (1, 4, 8) have been used in the denominator as estimates of the free plus nonspecifically bound ligand concentration. However, in patients with PSP, frontal perfusion has been reported to be significantly reduced (11), which might affect  $^{123}\text{I}$ -IBZM uptake. Furthermore, depressed patients with IPD appear to have greater frontal lobe dysfunction (12). In our study, we therefore used both the cerebellum and the occipital cortex as an area of reference because of the low dopamine D2 receptor density in these areas (13, 14).

The purpose of our study was to determine the variability of quantitative results of  $^{123}\text{I}$ -IBZM SPECT. First, studies using a brain phantom were performed in order to estimate count linearity in reconstructed transaxial SPECT images with respect to different  $^{123}\text{I}$  concentrations, scanning reproducibility and a wide range of radioactivity contrasts. Second,  $^{123}\text{I}$ -IBZM SPECT studies were performed in healthy controls and in patients with parkinsonian syndrome and analyzed by two observers in order to estimate interobserver variability and to choose the optimal parameter for estimating dopamine D2 receptor binding potential in the striatum.

## MATERIALS AND METHODS

### Instrumentation

SPECT imaging was performed with a high-sensitivity, high-resolution multidetector neuroSPECT system, the SME 810, fitted with 12 high-resolution, 800-hole collimators (Strichman Medical Equipment Inc., Medfield, MA). This system has an in-slice

---

Received Jan. 22, 1993; revision accepted Jul. 28, 1993.  
For correspondence or reprints contact: N.P.L.G. Verhoeff, MD, PhD, Singel 24, NL 2912 SL Nieuwerkerk aan den IJssel (ZH), The Netherlands.

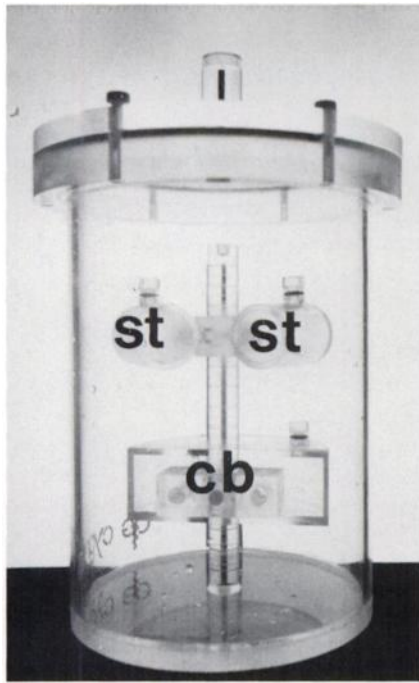


**FIGURE 1.** The perspex brain phantom designed with the aid of a stereotactic atlas (17). The relative position of the striatum and cerebellum chambers within the cylinder is shown.

spatial resolution of 6 mm (FWHM of a line source in air), a slice thickness of 1.2 cm and a sensitivity for  $^{99m}\text{Tc}$  of 315–520 kcts/sec/MBq/ml/slice (15,16). Data acquisition occurred on a  $128 \times 128$  matrix. Images were reconstructed in the highest resolution mode with one iteration using dedicated software (Strichman Medical Equipment Inc., version 2.65, 1990). Linear attenuation correction, based on an absorption length of 95 mm, was applied. In the phantom study, the attenuation contour corresponded to the phantom diameter of 14 cm (i.e., using a circle with a diameter of 85–90 pixels; pixel size was determined to be 0.164 mm). In the human studies, the attenuation contour corresponded to the diameter of the skull, as automatically estimated by the software.

### Phantom Studies

A cylindrical brain phantom was designed to contain various compartments that could be filled separately: two striatum, one cerebellum and the background (background), which consisted of the remaining part of the phantom (Fig. 1). The dimensions of the striatum and cerebellum were derived from a stereotactic brain atlas (17).

The phantom was 20 cm long and had an inner diameter of 14 cm. The cerebellum was a half-cylinder, with an inner diameter of 10 cm and a height of 3 cm. The two striatum were 4-cm long cylinders with an inner diameter of 2 cm. The compartmental volumes were 3079 ml for the whole phantom, 118 ml for the cerebellum and 13 ml each for the striatum. The longitudinal distance between the centers of the two striatum and the cerebellum was 6 cm.

Normally, about 3.5% of the injected activity of 185 MBq  $^{123}\text{I}$ -IBZM is taken up by the brain (2,18). Assuming a mean brain volume of 1450 ml, the concentration of  $^{123}\text{I}$  should then be 4.5 MBq/liter. The expected striatum-to-cerebellum ratio in clinical studies is about 2 (1,4).

Three experiments were performed. In Experiment 1, the striatum and cerebellum chambers were filled with a solution containing  $^{123}\text{I}$  in a concentration of 44.6 MBq/liter and sequential SPECT scans were obtained until the radioactivity had decayed to

0.8 MBq/liter. Background activity was chosen to be half of this concentration. The sequential scans were performed to measure linearity of the measured radioactivity concentration versus the real (or true) radioactivity concentration in a range of about 0.1–5 times the total radioactive counts expected clinically in the brain. The measured concentration was expressed in Strichman medical units (SMUs): 1 SMU = 100 Bq/ml, as specified by Strichman Medical Equipment Inc.

In the second experiment, the variability of the values for measured radioactivity concentration was determined from 20 repeated scans obtained with total raw counts/slice varying between about 40,000 to 1,800,000, which covers 0.1–2.25 times the clinically expected values (400,000–800,000 total raw counts/slice).

The third experiment was performed with striatum-to-background and cerebellum-to-background  $^{123}\text{I}$  concentration ratios varying from 1.2–10.8. The purpose was to determine the disparity between the real and measured contrast ratios striatum-to-background and cerebellum-to-background over a range from about 0.5 to 5 times those expected clinically. By comparing the measured striatum-to-background and cerebellum-to-background ratios, the effect of the size of the structure of interest on measured radioactivity concentration, i.e., a partial volume effect, could be estimated.

Regions of interest (ROIs) were drawn over the striatum and the cerebellum to correspond with the physical size and shape of the phantom structures. For the background, the ROI for the cerebellum was placed over the posterior area in the slice that contained the maximum striatum counts (Fig. 2a). Thus, the location of the ROI for the background was comparable to that of the occipital cortex in the human brain. The real and the calculated ratios were compared by computing recovery coefficients (RCs) (19,20):

$$\text{RC} = \frac{\text{measured ratio}}{\text{real ratio}} \times 100\%.$$

### Human Studies

Fifteen  $^{123}\text{I}$ -IBZM SPECT studies were performed on 15 healthy volunteers (9 male, 6 female; age 17–64 yr) and 36  $^{123}\text{I}$ -IBZM SPECT studies were performed in 28 patients with parkinsonian symptoms (19 male, 9 female; age 34–78 yr). Informed consent was obtained from volunteers and patients. The study was approved by the Medical Ethics Committee of the Academic Medical Centre.

Iodine-123-IBZM was synthesized as described previously (21). The specific activity was 222 GBq/ $\mu\text{mole}$ . A total activity of 185 MBq, containing about 0.8  $\mu\text{g}$  of IBZM, was administered intravenously. A multislice SPECT study was carried out at 120–180 min postinjection by acquiring 5-min slices between the cantomeatal line and the vertex at 10-mm spacing. At this time after injection, the ratio of specific binding versus nonspecific binding to the dopamine D2 receptors in the basal ganglia is at a maximum (4).

After reconstruction of the transverse slices, the two slices showing the highest striatal radioactivity were selected. ROIs were drawn around the striatum either: (1) manually using a 70% isocontour line of the SPECT signal (Fig. 2b) (1,4) or (2) by fitting predefined fixed regions, derived from a stereotactic brain atlas, and taking the outer contour of the striatum in the intercommissural plane ( $H \pm 0$ ) and in a plane 7 mm above and parallel to the intercommissural plane ( $H + 7$ ) (17) (Fig. 2c). With the manual

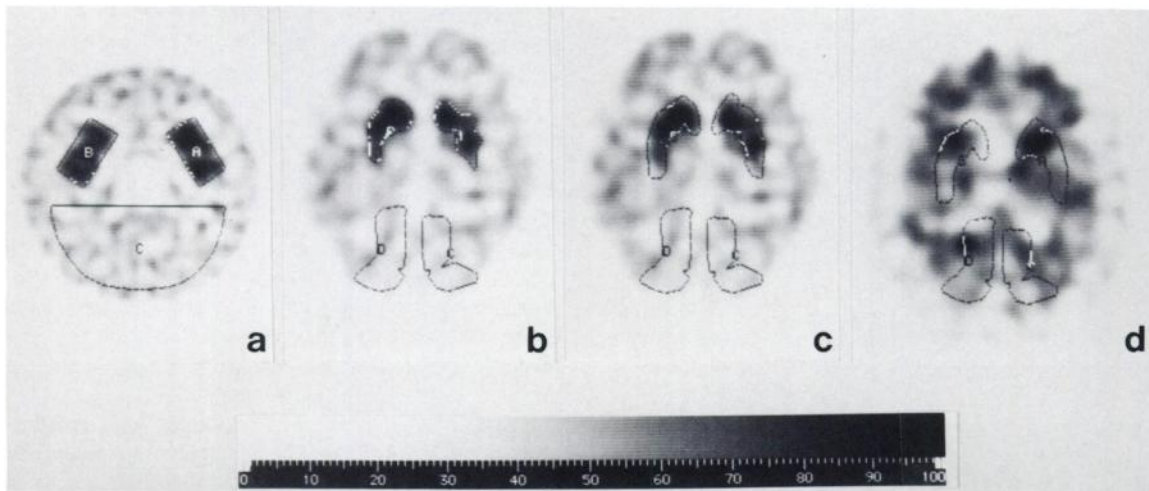


**FIGURE 2.** (a) SPECT image of the cylindrical brain phantom filled with  $^{123}\text{I}$  shows the fixed ROIs for the striatum (or basal ganglia and BGR) and background (extent of ROI based on the cerebellum). (b) Slice at 4 cm above and parallel to the cantomeatal line in a 62-yr-old female healthy volunteer at 150 min after injection of 185 MBq  $^{123}\text{I}$ -IBZM. The isocontour ROIs for the striatum and the fixed ROIs for the occipital cortex are shown. (c) The same slice in (b) shows the fixed ROIs for both the striatum and occipital cortex. (d) Slice at 4 cm above and parallel to the cantomeatal line in a 53-yr-old female patient with multiple system atrophy at 150 min after injection of 185 MBq  $^{123}\text{I}$ -IBZM. The fixed ROIs for the striatum and for the occipital cortex are shown. This image demonstrates the difficulty of selecting ROIs of the striatum based on isocontour lines.

method, the average area of the ROIs was  $404 \text{ mm}^2$  (s.d.  $46 \text{ mm}^2$ ;  $n = 15$ ) for the left striatum (striatum<sub>L</sub>) and  $406 \text{ mm}^2$  (s.d.  $51 \text{ mm}^2$ ;  $n = 15$ ) for the right striatum (striatum<sub>R</sub>). For the fixed ROIs at levels  $H \pm 0$  and  $H + 7$ , the areas were  $665$  and  $721 \text{ mm}^2$  for striatum<sub>L</sub> and  $678$  and  $709 \text{ mm}^2$  for striatum<sub>R</sub>, respectively. The cerebellum was used as a control region and was defined by a 50% isocontour line. The average area of this ROI was  $2630 \text{ mm}^2$  (s.d.  $436 \text{ mm}^2$ ;  $n = 15$ ). Another control region, derived from a neuro-anatomical atlas (22), was placed on the occipital cortex in the slices at the level of the striatum. The area of this ROI was  $751 \text{ mm}^2$  for the left occipital cortex and  $841 \text{ mm}^2$  for the right occipital cortex. The SMU values for the occipital cortex were taken as the mean of the values obtained in the left and right occipital cortex.

In some of the 28 patients with parkinsonian symptoms, the contrast between the striatum and the background was so low that isocontour ROIs could not be drawn reliably (see Fig. 2d). Therefore, only fixed ROIs were used in the patients' studies.

Ratios of the striatal SMUs to cerebellar SMUs and occipital SMUs, respectively, striatum-to-cerebellum and striatum-to-occipital cortex, were calculated. Also, left-to-right (L-to-R) SMU ratios were calculated from the striatum and the occipital cortex ROIs.

### Statistical Analysis

SMU variability measured in the repeated scans obtained in the second experiment of the phantom study and corrected for radioactive decay was expressed as the percent coefficient of variation (CV) (23).

The striatum and cerebellum SMUs, and striatum-to-cerebellum, striatum-to-occipital cortex and L-to-R ratios determined by two independent observers of the healthy volunteer studies and the patient studies were compared using Wilcoxon's signed rank sum test and Pearson's product-moment correlation coefficient. In this way, the statistical significance of the differences with respect to bias and level of association were assessed (23).

An estimate of the variability of the results of the two observers

was obtained from the percentage absolute difference divided by the mean measure of the observers:

$$\text{Relative \%Difference} = \frac{2 * |X_A - X_B|}{X_A + X_B} \times 100\%,$$

in which  $X_A$  and  $X_B$  are the values obtained by observers A and B. This estimates the mean as well as the maximum possible relative difference (either in a positive or in a negative direction) as a percentage of the value obtained by one observer.

In addition, the signed relative percentage of difference was calculated. This is the nonabsolute value of the parameter mentioned above. This was carried out for ratios that were optimal for quantification of dopamine D2 receptor binding potential and in which no bias was present according to Wilcoxon's signed rank test. In order to confirm that no bias was present, the 95% confidence interval of the mean signed relative difference was determined based on Student's distribution. The result should enclose the zero value (24).

Based on the 95% confidence intervals of the ratios of the SPECT data obtained in the healthy volunteers, limits were set in order to divide the patients into two groups: patients with reduced D2 receptor binding potential in the striatum and patients with normal D2 receptor binding potential. The two groups were categorized by attributing the values 1 and 2 to each group respectively, and the total squared observed difference  $d(u)$  and total squared chance difference  $c(u)$  were obtained. Then, epsilon ( $u$ ), the proportional reduction in squared difference compared to the chance squared difference, was calculated as:

$$\text{Upsilon} = u = \frac{c(u) - d(u)}{c(u)}.$$

When there are only two categories, as in our case, epsilon equals kappa (25). The kappa values of the ratios were compared to obtain the optimum ratio for comparison of patients and controls with respect to interobserver variability.

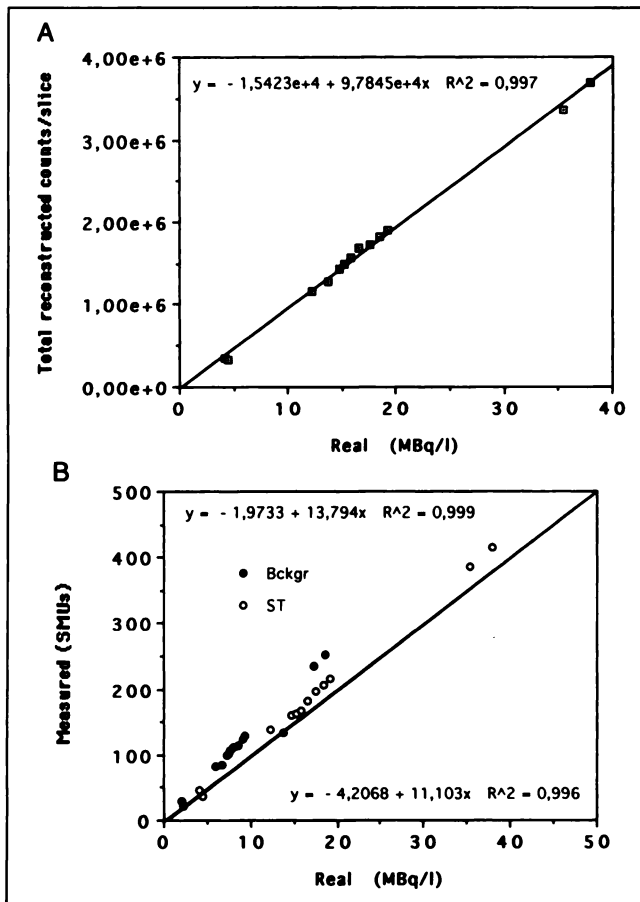


**FIGURE 3.** The linear relationship observed between the real radioactivity (in MBq/liter) in the brain phantom on the x-axis and the measured radioactivity (in SMUs) by the SME 810 for the whole slice (A) and for the striatum and background (B) on the y-axis.

## RESULTS

### Phantom Study

*Experiment 1.* A linear relationship between the real radioactivity and the measured radioactivity was obtained for the activity in the whole slice as well as that in the ROIs

**TABLE 2**  
RCs of Striatum-to-Background and Cerebellum-to-Background Ratios of <sup>123</sup>I Concentrations in the Cylindrical Brain Phantom Imaged with the SME810 SPECT Camera

Real ratio	Striatum-to-background RC (%)	Cerebellum-to-background RC (%)
1.2	88	86
1.3	83	85
1.5	81	81
1.6	85	81
1.8	82	81
2.0	81	78
3.8	76	79
5.4	76	73
10.8	105	95

for striatum, cerebellum and background (Fig. 3). The slopes of the linear fits for the ROIs were close to the expected value of 10 based on the SMUs specified by Strichman Medical Equipment Inc.

*Experiment 2.* Table 1 shows the CVs of the measured radioactivity concentration (in SMUs) in each ROI and the CVs of the ratios obtained from these values based on the 20 repeated measurements. An increase in CV with a decrease in total number of raw counts/slice can be observed for both ROIs and ratios. The second column represents the clinically relevant total number of raw counts for <sup>123</sup>I-IBZM SPECT (800,000 raw counts). For this count level, CVs obtained were 2.3% for the striatum, 1.9% for background, 1.5% for the striatum-to-background ratio and 2.7% for the striatum L-to-R ratio.

*Experiment 3.* The RCs for a range of real ratios of 1.2–5.4 between striatum or cerebellum and background were 75%–88% for the striatum-to-background ratios and 73%–86% for the cerebellum-to-background ratios (Table 2). Thus, in the clinically relevant part of the real ratios, the RCs were around 80%. For higher real ratios, the RCs showed a trend of decreasing. The RCs of about 100% for the real ratio of 10.8 were not in agreement with this trend.

**TABLE 1**

CVs from Different ROIs and Ratios Derived from Those ROIs, Obtained from SPECT Imaging of the Cylindrical Brain Phantom

ROI or ratio	Total raw counts per slice (1,000)					
	1,853	833	218	137	123	43
Striatum <sub>L</sub>	1.4	2.7	3.0	3.0	4.7	8.4
Striatum <sub>R</sub>	1.6	2.6	3.0	2.9	3.9	9.0
Striatum	1.2	2.3	1.7	2.4	3.2	5.1
Background	0.8	1.9	1.4	1.6	2.4	3.4
Striatum <sub>L</sub> -to-background	1.3	2.2	3.5	2.8	5.4	9.3
Striatum <sub>R</sub> -to-background	1.7	1.8	3.3	3.3	4.1	9.1
Striatum-to-background	1.2	1.5	2.4	2.4	3.8	6.4
Striatum L-to-R	2.0	2.7	4.9	3.7	5.7	12.8

Each CV is based on SMUs obtained in 20 repeat scans using the SME810 SPECT system with a striatum or cerebellum-to-background ratio of <sup>123</sup>I concentration of 2.05.

**TABLE 3**  
Interobserver Comparison of Isocontour ROIs for the Striatum and Cerebellum and Fixed ROIs for the Occipital Cortex Derived from 15 <sup>123</sup>I-IBZM SPECT Studies in 15 Healthy Volunteers

ROI	Observer 1 values		Observer 2 values		%Relative difference		Wilcoxon p	Pearson	
	Mean	s.d.	Mean	s.d.	Mean	s.d.		r	p
Striatum <sub>L</sub>	78	20	78	21	2	2	0.57	0.99	<0.01
Striatum <sub>R</sub>	78	20	77	20	3	2	0.21	0.99	<0.01
Cerebellum	40	10	38	10	6	4	<0.01	0.99	<0.01
Occipital cortex	35	10	35	10	2	3	0.11	0.99	<0.01
Striatum <sub>L</sub> -to-cerebellum	1.94	0.16	2.07	0.17	7	4	<0.01	0.88	<0.01
Striatum <sub>R</sub> -to-cerebellum	1.94	0.18	2.05	0.19	6	4	<0.01	0.89	<0.01
Striatum-to-cerebellum	1.94	0.16	2.06	0.17	6	4	<0.01	0.88	<0.01
Striatum <sub>L</sub> -to-occipital cortex	2.25	0.12	2.22	0.14	2	2	0.06	0.91	<0.01
Striatum <sub>R</sub> -to-occipital cortex	2.26	0.20	2.20	0.21	3	3	<0.01	0.94	<0.01
Striatum-to-occipital cortex	2.26	0.15	2.21	0.17	2	2	<0.01	0.93	<0.01
Striatum L-to-R	1.00	0.06	1.01	0.07	2	1	0.17	0.93	<0.01

Values for radioactivity concentration in the ROIs are expressed in SMUs.

### Healthy Volunteers

SMU variability values obtained with fixed and isocontour ROIs in the 15 volunteers were similar (Tables 3 and 4). In the 15 volunteers, the mean relative difference was 6% for the cerebellum, but only 2% for the occipital cortex. Furthermore, the mean relative difference for the striatum decreased from 2%–3% to 1% when fixed ROIs were used instead of isocontour ROIs. Due to the larger variability in the cerebellum, the variability in the striatum-to-cerebellum ratios was larger (mean relative difference 6%–7%) than the variability of the striatum-to-occipital cortex ratios (mean relative difference only 2–3%).

The difference between the two observers was statistically significant for the cerebellum and, consequently, for the ratios with the cerebellum in the denominator. Also, the striatum<sub>R</sub>-to-occipital cortex and striatum-to-occipital cortex ratios were significantly different when isocontour lines were used for the striatum, but not when fixed ROIs

were used. A linear association between the data of both observers was present in all cases ( $r = 0.85$ – $1.00$ ;  $p < 0.01$ ).

For the striatum-to-occipital cortex ratios with fixed ROIs for the striatum, this study showed a low variability, no significant difference between observers and a highly significant correlation. The lack of interobserver bias using Wilcoxon's signed rank sum test was confirmed from the 95% confidence interval of the mean percentage signed relative difference enclosing zero (Table 5). Most interobserver variability occurred within 9% in either the positive or the negative direction.

### Patients with Parkinsonian Syndrome

In the 28 patients with parkinsonian symptoms, only the fixed ROIs for the striatum were used because isocontour lines could not be obtained reliably in those patients with a low uptake in the striatum (Fig. 2d). Table 6 shows the

**TABLE 4**  
Interobserver Comparison of Fixed ROIs for the Striatum and Occipital Cortex and Isocontour ROIs for the Cerebellum Derived from 15 <sup>123</sup>I-IBZM SPECT Studies in 15 Healthy Volunteers

ROI	Observer 1 values		Observer 2 values		%Relative difference		Wilcoxon p	Pearson	
	Mean	s.d.	Mean	s.d.	Mean	s.d.		r	p
Striatum <sub>L</sub>	66	17	67	17	1	1	0.10	1.00	<0.01
Striatum <sub>R</sub>	67	17	67	17	1	1	0.25	1.00	<0.01
Striatum <sub>L</sub> -to-cerebellum	1.65	0.13	1.77	0.15	7	4	<0.01	0.87	<0.01
Striatum <sub>R</sub> -to-cerebellum	1.66	0.13	1.77	0.16	7	4	<0.01	0.88	<0.01
Striatum-to-cerebellum	1.65	0.12	1.77	0.15	7	4	<0.01	0.87	<0.01
Striatum <sub>L</sub> -to-occipital cortex	1.92	0.10	1.90	0.12	2	3	0.35	0.85	<0.01
Striatum <sub>R</sub> -to-occipital cortex	1.93	0.15	1.91	0.17	3	3	0.27	0.92	<0.01
Striatum-to-occipital cortex	1.93	0.12	1.91	0.14	2	3	0.25	0.89	<0.01
Striatum L-to-R	1.00	0.05	1.00	0.05	1	1	0.48	0.97	<0.01

Radioactivity concentration values are expressed in SMUs.

**TABLE 5**  
Level of Agreement of Striatum-to-Occipital Cortex Ratios Based on Fixed ROIs Derived from 15 <sup>123</sup>I-IBZM SPECT Studies in 15 Healthy Volunteers

ROI	%Signed relative difference 95% confidence interval	%Mean signed relative difference 95% confidence interval
Striatum <sub>L</sub> -to-occipital cortex	-6.1-8.1	-0.8-2.8
Striatum <sub>R</sub> -to-occipital cortex	-6.2-8.8	-0.7-3.2
Striatum-to-occipital cortex	-6.3-8.7	-0.8-3.2

The 95% confidence intervals were based on Student's distribution with  $t_{1,4} = 2.145$  (23).

results from the 36 SPECT studies performed in these patients.

The variability in all ROIs was greater in the patients than in the volunteers (mean relative differences: 9% versus 6% for the cerebellum, 2%-4% versus 1% for the striatum and 4%-5% versus 2%-3% for the occipital cortex, respectively). Consequently, the variability in the ratios was larger (9% versus 7% for the striatum-to-cerebellum ratios and 4%-5% versus 2%-3% for the striatum-to-occipital cortex ratios).

A linear association between the data of both observers was present in all cases ( $r = 0.49-1.00$ ;  $p < 0.01$ ). The correlation of the striatum-to-occipital cortex ratios ( $r = 0.92-0.96$ ) was better than that of the striatum-to-cerebellum ratios ( $r = 0.74-0.76$ ).

Interobserver bias was present for the striatum-to-occipital cortex ratios according to Wilcoxon's signed rank sum test (Table 6). The bias could not be confirmed from the 95% confidence interval of the mean signed relative

**TABLE 7**  
Level of Agreement of Striatum-to-Occipital Cortex Ratios Based on Fixed ROIs Derived from 36 <sup>123</sup>I-IBZM SPECT Studies in 28 Patients with Parkinsonism

ROI	%Relative difference 95% confidence interval	%Mean signed relative difference 95% confidence interval
Striatum <sub>L</sub> -to-occipital cortex	-5.5-15.8	-0.4-4.3
Striatum <sub>R</sub> -to-occipital cortex	-4.7-13.4	-0.7-3.4
Striatum-to-occipital cortex	-4.3-13.0	-0.1-3.7

differences, but the lower border of the confidence interval was very close to zero (Table 7). Using a conservative approach, the percentage relative differences were taken as a worst case in which all differences were in the same direction. Most of the interobserver variability occurred within 16%.

#### Reliability of Classification of Patients with Parkinsonian Syndrome

Table 8 shows the ranges and confidence intervals for the ratios obtained from the volunteers by the two observers. Based on the lower limits, the patients were divided into two groups: decreased D2 receptor binding potential (striatum-to-cerebellum ratios  $\leq 1.5$  or striatum-to-occipital cortex ratios  $\leq 1.8$ ) or normal or increased D2 receptor binding potential (striatum-to-cerebellum ratios  $> 1.5$  or striatum-to-occipital cortex ratios  $> 1.8$ ). Group 1 was given the value 1 and Group 2 was given the value 2. The resulting epsilon values, equal to kappa for these two categories, are given in Table 9. With epsilon as a measure of agreement, interobserver agreement for the striatum-to-cerebellum ratios was only moderate, whereas the agree-

**TABLE 6**  
Interobserver Comparison of Fixed ROIs for the Striatum and Occipital Cortex and Isocontour ROIs for the Cerebellum Derived from 36 <sup>123</sup>I-IBZM SPECT Studies in 28 Patients with Parkinsonism

ROI	Observer 1 values		Observer 2 values		%Relative difference		Wilcoxon p	Pearson	
	Mean	s.d.	Mean	s.d.	Mean	s.d.		r	p
Striatum <sub>L</sub>	57	22	56	21	4	4	<0.01	0.99	<0.01
Striatum <sub>R</sub>	57	20	56	20	2	3	<0.01	1.00	<0.01
Cerebellum	36	13	34	12	9	11	<0.01	0.95	<0.01
Occipital cortex	33	12	34	12	4	4	0.62	0.99	<0.01
Striatum <sub>L</sub> -to-cerebellum	1.62	0.28	1.65	0.34	9	10	0.48	0.76	<0.01
Striatum <sub>R</sub> -to-cerebellum	1.61	0.29	1.66	0.36	9	12	<0.01	0.74	<0.01
Striatum-to-cerebellum	1.62	0.28	1.66	0.35	9	11	0.22	0.76	<0.01
Striatum <sub>L</sub> -to-occipital cortex	1.71	0.29	1.68	0.28	5	5	<0.01	0.92	<0.01
Striatum <sub>R</sub> -to-occipital cortex	1.71	0.33	1.68	0.31	4	4	0.04	0.96	<0.01
Striatum-to-occipital cortex	1.71	0.30	1.68	0.29	4	4	0.03	0.96	<0.01
Striatum L-to-R	1.01	0.07	1.00	0.06	4	5	0.24	0.49	<0.01

Radioactivity concentration values are expressed in SMUs.

**TABLE 8**

Range and Confidence Intervals of Striatum-to-Cerebellum and Striatum-to-Occipital Cortex Ratios with the Striatum and Occipital Cortex Based on Fixed ROIs and the Cerebellum on Isocontour ROIs Derived from 15 <sup>123</sup>I-IBZM SPECT Studies in 15 Healthy Volunteers

Ratio		Range	95% confidence interval
Striatum <sub>L</sub> -to-cerebellum	Obs. 1	1.39–1.85	1.58–1.72
	Obs. 2	1.55–2.02	1.69–1.86
Striatum <sub>R</sub> -to-cerebellum	Obs. 1	1.37–1.83	1.59–1.73
	Obs. 2	1.52–2.10	1.68–1.86
Striatum-to-cerebellum	Obs. 1	1.42–1.81	1.59–1.72
	Obs. 2	1.58–2.06	1.69–1.86
Striatum <sub>L</sub> -to-occipital cortex	Obs. 1	1.78–2.11	1.87–1.97
	Obs. 2	1.67–2.11	1.84–1.97
Striatum <sub>R</sub> -to-occipital cortex	Obs. 1	1.74–2.38	1.85–2.01
	Obs. 2	1.69–2.38	1.81–2.00
Striatum-to-occipital cortex	Obs. 1	1.76–2.25	1.86–1.99
	Obs. 2	1.68–2.25	1.83–1.98

ment for the striatum-to-occipital cortex ratios was very good.

**DISCUSSION**

Phantoms, such as the one we used in this study, have been developed by others for similar purposes (19,26,27). The linearity between the real radioactivity concentration in the brain phantom and the radioactivity concentration (in SMUs) measured with the SME 810 confirmed previous findings using the same SPECT system and software (28). The CVs for the values obtained for the different ROIs and ratios for repeated scanning of the phantom at the level of the striatum were in the range of 0.8%–12.8%. This is very similar to the 10% variation due to technical factors reported for a PET system with the same resolution as the

**TABLE 9**

Upsilon, the Proportional Reduction in Squared Difference Between the Two Observers, Compared to the Chance Squared Difference for Two Patient Categories with Values 1 (Striatum-to-Cerebellum Ratios ≤ 1.5 or Striatum-to-Occipital Cortex Ratios ≤ 1.8) and 2 (Striatum-to-Cerebellum Ratios > 1.5 or Striatum-to-Occipital Cortex Ratios > 1.8)

Ratio	Upsilon (kappa)	Interpretation of agreement (24)
Striatum <sub>L</sub> -to-cerebellum	0.56	Moderate
Striatum <sub>R</sub> -to-cerebellum	0.57	Moderate
Striatum-to-cerebellum	0.68	Good
Striatum <sub>L</sub> -to-occipital cortex	0.82	Very good
Striatum <sub>R</sub> -to-occipital cortex	0.81	Very good
Striatum-to-occipital cortex	0.88	Very good

Upsilon values may be used as kappa (25).

SME 810 (6 mm FWHM using a line source) (19), as well as for PET in general (29).

The 80% RCs from our study agree well with the 75% RC reported by Bendriem et al. (19) for zero background concentration. For realistic striatum-to-background ratios, Bendriem et al. (19) reported RCs of 72% for a large ROI of >75 pixels and 80% for a small ROI of only five pixels. Our RC values of 76% and 79% for the striatum-to-background and cerebellum-to-background ratios, respectively, for a real ratio of 3.8 (Table 2) are comparable to their findings. Scatter correction increased the RC values by 9% in the study of Bendriem et al. (19). No extra scatter correction was performed in our study. The results, however, show that comparable results can be obtained for high sensitivity PET and SPECT systems with similar spatial resolution.

The high RC reported by Bendriem et al. (19) using a smaller ROI over the center of the structure of interest was also observed by Hatazawa et al. (27), who used a PET scanner with a spatial resolution of 7 mm (FWHM) and a 7-mm diameter circular ROI placed over the center of a 30-mm diameter hot phantom. They observed that when a 30-mm ROI was used instead of a 7-mm ROI, the RC was only about 50%. However, in our study with ROIs the same physical size as the striatum (20 × 40 mm), the RCs were considerably higher.

High RCs were obtained in our study for a real striatum or cerebellum over a background ratio of 10.8. These high RCs do not fit the trend of decreasing RCs with increasing real ratios in our study, the reported decrease in RC with increasing contrast (19) or a strong partial volume effect (27). They might be due to contrast enhancement of the filters used in the SME version 2.65 software.

Ideally, anatomical (CT, MRI) and functional (PET, SPECT) images should be available for direct comparison (30). Several methods have been developed to match anatomical and functional image data of the brain (31–33). Some of these have already been implemented for SPECT (34) and PET studies (35). Such comparisons may provide the opportunity to make better corrections for partial volume effects, especially with respect to atrophy.

Without this possibility, we used fixed ROIs based on a stereotactic atlas superimposed on and adjusted to the SPECT images. Based on these ROIs, ratios of total binding to nonspecific binding were calculated in order to estimate the dopamine D2 receptor binding potential in the striatum. We did not attempt to obtain K<sub>d</sub> and B<sub>max</sub> values because complicated protocols, including arterial sampling and scanning with different specific activities of the radioligand, are necessary. Assessment of group discrimination and disease progression does not necessarily benefit from the optimization methods of parameters traditionally used in absolute quantification with PET (36).

We found that fixed ROIs are preferable to isocontour ROIs for the comparison of healthy volunteers and patients with parkinsonian syndrome using <sup>123</sup>I-IBZM SPECT. In our opinion, fixed ROIs are absolutely necessary in those

patients who display a decreased uptake of  $^{123}\text{I}$ -IBZM in the striatum because isocontour ROIs cannot be drawn reliably. Furthermore, in the volunteer studies, the use of fixed ROIs resulted in fewer differences between the two observers. Several other groups have already implemented fixed ROIs derived from stereotactic brain atlases for analysis of SPECT (15) and PET studies (20). The use of a reference atlas has been highly recommended by Rapoport (29) for PET. The areas of our isocontour and fixed ROIs for the striatum were similar to those of the ROIs selected by Tedroff et al. (37). Although we drew a large ROI for the cerebellum, it proved to be less reliable compared to the occipital cortex based on the larger interobserver variability. This could be improved by also selecting a fixed ROI for the cerebellum.

In the group of patients with parkinsonian symptoms, both the cerebellum and the striatum values were significantly different between observers. This may reflect the difficulty in defining the exact location and extent of the striatum. Nevertheless, the striatum-to-cerebellum ratios were not significantly different between the two observers. This was probably due to the large variability of these ratios. In the occipital cortex, no significant differences were obtained, as in the volunteers. However, even though the variability of the striatum-to-occipital cortex ratios was smaller, significant differences were observed due to different values for the striatum.

In conclusion, striatum-to-occipital cortex ratios based on fixed ROIs provided the best quantitative estimation for the dopamine D2 receptor binding potential of the striatum because they showed the smallest interobserver variability. Indeed, the  $\epsilon$  values indicated that the agreement between the observers was very good. Comparative studies of healthy volunteers and patients may well be superior when performed by a single observer rather than by several observers. In case different observers contribute to a study, wider variability margins have to be considered for values obtained both in volunteers and in patients. From our study, use of striatum-to-occipital cortex ratios based on fixed ROIs to estimate D2 receptor binding potential in the striatum as measured with  $^{123}\text{I}$ -IBZM SPECT resulted in margins of 9% for volunteers and 16% for patients. Margins derived from interobserver variability studies will become increasingly important if SPECT results are directly applied to clinical outcome and patient management.

## ACKNOWLEDGMENTS

The authors would like to express their gratitude to Cygne B.V. for manufacturing the brain phantom and for providing the  $^{123}\text{I}$  and  $^{123}\text{I}$ -IBZM. The authors thank P.M.M. Bossuyt, PhD, clinical epidemiologist, for advice regarding statistical analysis and G.J. Boer, PhD, for additional comments.

## REFERENCES

- Costa DC, Verhoeff NPLG, Cullum ID, et al. In vivo characterisation of a 3-iodo-6-methoxybenzamide  $^{123}\text{I}$  in humans. *Eur J Nucl Med* 1990;16:813-816.
- Kung HF, Alavi A, Chang W, et al. In vivo SPECT imaging of CNS D-2 dopamine receptors: initial studies with iodine-123-IBZM in humans. *J Nucl Med* 1990;31:573-579.
- Verhoeff NPLG, Bobeldijk M, Feenstra MGP, et al. In vitro and in vivo D<sub>2</sub>-dopamine receptor binding with ( $^{123}\text{I}$ )IBZM in rat and human brain. *Nucl Med Biol* 1991;18:837-846.
- Verhoeff NPLG, Brücke T, Podreka I, Bobeldijk M, Angelberger P, Van Royen EA. Dynamic SPECT in two healthy volunteers to determine the optimal time for in vivo D2 dopamine receptor imaging with  $^{123}\text{I}$ -IBZM using the rotating gamma camera. *Nucl Med Commun* 1991;12:687-697.
- Seibyl JP, Woods SW, Zoghbi SS, et al. Dynamic SPECT imaging of dopamine D2 receptors in human subjects with iodine-123-IBZM. *J Nucl Med* 1992;33:1964-1971.
- Van Royen EA, Verhoeff NPLG, Speelman JD, Wolters ECh, Kuiper MA, Janssen AGM. Multiple system atrophy and progressive supranuclear palsy. Diminished striatal D<sub>2</sub> dopamine receptor activity demonstrated by  $^{123}\text{I}$ -IBZM single photon emission computed tomography. *Arch Neurol* 1993;50:513-516.
- Verhoeff NPLG, Speelman JD, Van Royen EA, De Jong JMBV. In vivo dopamine D2-receptor imaging with I-123 iodobenzamide SPECT in patients with multiple system atrophy [Abstract]. *Eur J Nucl Med* 1990;16:520.
- Brücke T, Podreka I, Angelberger P, et al. Dopamine D<sub>2</sub> receptor imaging with SPECT: studies in different neuropsychiatric disorders. *J Cereb Blood Flow Metab* 1991;11:220-228.
- Schwarz J, Tatsch K, Arnold G, et al.  $^{123}\text{I}$ -iodobenzamide SPECT predicts dopaminergic responsiveness in patients with de novo parkinsonism. *Neurology* 1992;42:556-561.
- Ford I, McColl JH, McCormack AG, McCrory SJ. Statistical Issues in the analysis of neuroimages. *J Cereb Blood Flow Metab* 1991;11(suppl 1):A89-A95.
- Johnson KA, Sperling RA, Holman BL, Nagel JS, Growdon JH. Cerebral perfusion in progressive supranuclear palsy. *J Nucl Med* 1992;33:704-709.
- Cummings JL. Depression and Parkinson's disease: a review. *Am J Psychiatry* 1992;149:443-454.
- Camps M, Cortés R, Gueye B, Probst A, Palacios JM. Dopamine receptors in the human brain: autoradiographic distribution of D2 sites. *Neuroscience* 1989;28:275-290.
- Lidow MS, Goldman-Rakic PS, Rakic P, Innis RB. Dopamine D2 receptors in the cerebral cortex: distribution and pharmacological characterization with ( $^3\text{H}$ ) raclopride. *Proc Natl Acad Sci USA* 1989;86:6412-6416.
- Ebmeier KP, Dougall NJ, Austin MPV, et al. The split-dose technique for the study of psychological and pharmacological activation with the cerebral blood flow marker exametazime and single photon emission computed tomography (SPECT): reproducibility and rater reliability. *Int J Meth Psych Res* 1991;1:27-38.
- George MS, Ring HA, Costa DC, Ell PJ, Kouris K, Jarritt PH. *Neuroactivation and neuroimaging with SPET*. London, UK: Springer-Verlag Ltd.; 1991:42.
- Schaltenbrand G, Wahren W. *Atlas for stereotaxy of the human brain*, 2nd edition. Stuttgart, BRD: George Thieme; 1977.
- Verhoeff NPLG, Van Royen EA, Horn J, et al. Whole body distribution of I-123 iodobenzamide in six healthy human volunteers [Abstract]. *J Nucl Med* 1991;32:1018.
- Bendriem B, Dewey SL, Schlyer DJ, Wolf AP, Volkow ND. Quantitation of the human basal ganglia with positron emission tomography: a phantom study of the effect of contrast and axial positioning. *IEEE Trans Med Imaging* 1991;10:216-222.
- Bohm C, Greitz T, Seitz R, Eriksson L. Specification and selection of regions of interest (ROIs) in a computerized brain atlas. *J Cereb Blood Flow Metab* 1991;11(suppl 1):A64-A68.
- Bobeldijk M, Verhoeff NPLG, Vekemans JAJM, et al. A simple and high-yield synthesis of (S)-BZM, (R)-BZM and (S)-IBZM for the preparation of ( $^{123}\text{I}$ )-IBZM. *J Lab Compol Radiopharm* 1990;28:1247-1256.
- Matsui T, Hirano A. *An atlas of the human brain for computerised tomography*. Stuttgart: Gustav Fischer Verlag; 1978.
- Armitage P, Berry G. *Statistical methods in medical research*, 2nd edition. Oxford, UK: Blackwell Scientific Publ.; 1987:40-41, 150-152, 410-414, 510-511.
- Brennan P, Silman A. Statistical methods for assessing observer variability in clinical measures. *BMJ* 1992;304:1491-1494.
- Schouten HJA. *Statistical measurement of interobserver agreement. Analysis of agreements and disagreements between observers*. PhD thesis. Erasmus University Rotterdam. Utrecht, Netherlands: Elinkwijk B.V.; 1985: 1-35.
- Hall H, Högberg T, Halldin C, et al. NCQ 298, a new selective iodinated

- salicylamide ligand for the labelling of dopamine D2 receptors. *Psychopharmacology* 1991;103:6-18.
27. Hatazawa J, Hatano K, Ishiwata K, et al. Measurement of D2 dopamine receptor-specific carbon-11-YM-09151-2 binding in the canine brain by PET: importance of partial volume correction. *J Nucl Med* 1991;32:713-718.
  28. Innis RB, Al-Tikriti MS, Zoghbi SS, et al. SPECT imaging of the benzodiazepine receptor: feasibility of in vivo potency measurements from stepwise displacement curves. *J Nucl Med* 1991;32:1754-1761.
  29. Rapoport SI. Discussion of PET workshop reports, including recommendations of PET data analysis working group. *J Cereb Blood Flow Metab* 1991;11(suppl 1):A140-A146.
  30. Mazziotta JC, Pelizzari CC, Chen GT, Bookstein FL, Valentino D. Region of interest issues: the relationship between structure and function in the brain. *J Cereb Blood Flow Metab* 1991;11(suppl 1):A51-A56.
  31. Pelizzari CA, Chen GTY, Spelbring DR, Weichselbaum RR, Chen CT. Accurate three-dimensional registration of CT, PET, and/or MR images of the brain. *J Comput Assist Tomogr* 1989;13:20-26.
  32. Evans AC, Marrett S, Torrescorzo J, Ku S, Collins L. MRI-PET correlation in three dimensions using a volume-of-interest (VOI) atlas. *J Cereb Blood Flow Metab* 1991;11(suppl 1):A69-A78.
  33. Van den Elsen PA, Viergever MA, Van Huffelen AC, Van der Meij W, Wieneke GH. Accurate matching of electromagnetic dipole data with CT and MR images. *Brain Topography* 1991;3:425-432.
  34. Holman BL, Zimmerman RE, Johnson KA, et al. Computer-assisted superimposition of magnetic resonance and high-resolution technetium-99m-HMPAO and thallium-201 SPECT images of the brain. *J Nucl Med* 1991;32:1478-1484.
  35. Müller-Gärtner HW, Links JM, Prince JL, et al. Measurement of radiotracer concentration in brain gray matter using positron emission tomography: MRI-based correction for partial volume effects. *J Cereb Blood Flow Metab* 1992;12:571-583.
  36. Strother SC, Liow JS, Moeller JR, Sidtis JJ, Dhawan VJ, Rottenberg DA. Absolute quantitation in neurological PET: do we need it? *J Cereb Blood Flow Metab* 1991;11(suppl 1):A3-A16.
  37. Tedroff J, Aquilonius SM, Hartvig P, Bredberg E, Bjurling P, Langström B. Cerebral uptake and utilization of therapeutic [ $\beta$ - $^{11}\text{C}$ ]-1-DOPA in Parkinson's disease measured by positron emission tomography. Relation to motor response. *Acta Neurol Scand* 1992;85:95-102.